**The Journal of Medicinal Plants and By-products**

**Original Article**

# Anti-Catalyze Enzyme, Anti-biofilm, Antibacterial Effectiveness of Calcium Bio-Synthesized Nanoparticles from *Pseudomonas aeruginosa*

Ismail Jmia Abbass

*Department of Biology, College of Education, Quran, University of Basrah, Basrah, Iraq*

*Corresponding author: Email: ismail.abbs@uobasrah.edu.iq

Article History: Received 23 February 2026/Accepted in revised form 13 April 2026


## ABSTRACT

Nanotechnology is a crucial modern science focused on the creation of small-sized particles with significant effectiveness, particularly in health applications. There are three primary methods for synthesizing nanoparticles: physical, chemical, and biological. The biological method is preferred due to its environmentally friendly nature, low cost, and minimal equipment requirements. This study utilized the biological method to synthesize calcium nanoparticles (CaNPs) using the supernatant solution from *Pseudomonas aeruginosa* bacteria isolated from soil. The nanoparticles were characterized microscopically, morphologically, and molecularly. Characterization techniques included colorimetric analysis, UV-visible spectrophotometry, FT-IR, and scanning electron microscopy (SEM), all of which confirmed the successful synthesis of CaNPs. Biofilm-forming bacteria were identified using Congo red and microtiter plate methods, revealing that the pathogenic isolates *E. coli*, *K. pneumoniae*, *P. aeruginosa*, *and S. aureus* exhibited a strong ability to form biofilms. Additionally, the effectiveness of the synthesized nanoparticles in inhibiting biofilms formed by these pathogenic bacteria was tested, demonstrating their antibacterial properties and ability to inhibit catalase enzyme activity.

**Keywords:** UV, spectroscopy, CaNPs, *Pseudomonas aeruginosa,* Anti-biofilm

## INTRODUCTION

Nanotechnology is recognized as a significant modern research field with a profound impact on medical sciences. It has emerged as a multidisciplinary science, offering solutions to various challenges. One key reason for the use of copper in nanosynthesis is its high conductivity and non-oxidizing properties, making it a viable alternative to gold and silver [1-3]. The metallic nanoparticles of calcium (CaNPs) are important in various applications due to their unique chemical and physical properties, including antibacterial effects attributed to their high surface area. Their small size allows calcium nanoparticles to penetrate the walls of microorganisms. Additionally, calcium nanoparticles have applications in other biological fields, such as pharmaceuticals and environmental purification [4, 5]. The synthesis of calcium nanoparticles (CaNPs) is crucial for inhibiting both Gram-negative and Gram-positive bacteria. Additionally, these nanoparticles play a significant role in absorption and adsorption, effectively serving as an antidote to microbial activities [6]. The aim of this study is to synthesize nanoparticles from Calcium salt and evaluate the effectiveness of these particles in inhibiting biofilms formed by pathogenic bacteria. And as antibacterial and anti-catalase enzyme.

## MATERIALS AND METHODS

### Sample Collection

Samples were collected from various soil types, including sewage, soil from the banks of the Tigris and Euphrates rivers, agricultural soil, and oil-polluted soil. These samples were gathered from the northern region of Basra, particularly in the districts of Al-Qurna and Al-Madinah, and then transported to the laboratory.

### Isolation of Samples

Samples were grown on culture media (nutrient agar, blood agar, and MacConky agar). Through these mediums, bacteria are grown and then differentiated.

### Bacterial Diagnosis

### Microscopic Diagnosis

The bacteria were examined under a microscope to identify whether they were Gram-positive or Gram-negative and to observe their shapes.

### Phenotypic Diagnosis

Bacterial isolates grown on different media are identified by the color of the colonies, the shape of their edges, their height, and the size of the colonies.

### Biochemical Diagnosis

Biochemical tests were performed to diagnose the bacteria: methyl red, catalase, oxidase, citrate, urease, and indole.

### Molecular Diagnosis

### DNA Extraction

The DNA of *Pseudomonas aeruginosa* bacteria used in the biosynthesis of CaNP nanoparticles was extracted by the Presto TMMinig DNA Bacteria Kit protocol provided by Geneaid company.

### Electrical Deportation

The electrophoresis process was carried out according to previous research [7]

### Polymerase Chain Reaction (PCR)

The polymerase chain reaction (PCR) was performed on the DNA extracted from the purified bacterial isolates using the Primax PCR mix, and the Sequence of primers used in the study as shown in the table 1.

**Table 1** Sequence of primers used in the study

| Gene | Primer sequence (5-3) | bp | | Source |
|---|---|---|---|---|
| *16SrRNA* | 5`AGAGTTTGATCMTGGCTCAG `(20mer) | F | 1500 | (Burghal) *et al* 2015 |
| | 5 ` TACGGTACCTTGTTACGACTT3`(22mer) | R | | |

### Synthesis of Extracellular Nanoparticles from P. *aeruginosa* Bacteria

### Preparation of Suspension for *P aeruginosa.* Bacteria

The P.*aeruginosa* bacteria were cultured in nutrient broth medium and incubated in a shaking incubator at 150 rpm and 37 °C for 48 hours to form biomass. Afterward, the culture was centrifuged at 6000 rpm to remove the bacteria, resulting in a bacterial suspension that was stored at 4 °C until needed.

### Synthesis of Calcium Nanoparticles (CaNPs)

Nanoparticles were synthesized based on method [8]. 0.100 g of calcium oxide was dissolved in 100 ml of sterile distilled water, resulting in a concentration of 0.01 mm. This solution was stored until needed. Subsequently, 100 ml of the calcium oxide solution was mixed with 100 ml of a suspension of P. *aeruginosa* bacteria, and a color change was observed.

### Nanoparticle purification

The synthesized nanoparticles were washed three times with distilled deionized water for 15 minutes each time. The resulting mixture was then centrifuged at 6000 rpm to eliminate any suspended sediments. Afterward, the nanoparticles were dried in a hot oven at 100 °C for 3 hours. They were now ready for use and for further tests to determine their size, shape, and composition.

### Devices and Techniques Used in the Characterization of CaNPs, Nanoparticles

### Chromatic Variation

The first indication that the biosynthesis of nanoparticles has occurred is the chromatic variation of the solution.

### UV-vis Spectroscopy

A 3 ml sample of the bacterial supernatant solution from the *P.aeruginosa* culture was placed in the device, and its absorbance was measured. After observing a color change, another 3 ml sample of the solution was taken, and the device was incubated. The absorbance was measured again and compared to that of the initial bacterial supernatant.

### FT-IR Spectrometer

A FT-IR 4600 spectrometer was utilized to accurately and clearly detect the functional groups present in the bacterial supernatant solution after reduction by mineral salts, with a resolution of 4 $cm^{-1}$. To prepare the sample, 0.1 mg of nanomaterials were weighed and dissolved in 10 ml of dimethyl sulfoxide. The solution was then placed in an ultrasonic device for 16 minutes to thoroughly homogenize the nanomaterials with the solvent. Following this, a small aliquot (5–10 µL) was pipetted onto the crystal lens, checked for bubbles, and pressed with the pressure arm for analysis [9].

### Scanning Electron Microscope (SEM)

Another method for examining nanoparticles is the use of a scanning electron microscope (SEM) for surface imaging. This technique reveals the shape and size distribution of nanoparticles and allows for analysis of their structural characteristics. It also provides crucial information about the degree of agglomeration and the purity of the formed particles. Modern SEM devices can accurately determine the shape of nanoparticles smaller than 15 nanometers. For the examination, the nanomaterial is placed on the SEM plate and then coated with a layer of gold to ensure electrical conductivity [10].

### Detection of Biofilm-forming Bacterial Isolates

### 2.6.1 Use of Congo Red Agar Medium

This method was used according to what was stated in previous research [11] and evaluated using bacterial specimens obtained from Qurna College's Microbiology Laboratory. Efficacy against*. E. coli, K. penumonae, P. aeruginosa,* and *S. aureus*.

### Delection of Biofilm Formation by Microtiter Plate (MTP)

The bacterial isolates forming biofilms were detected according to previous research [12] using the multiscan Go device. Then, the absorbance of all the holes was calculated using the same device at a wavelength of (630) nanometers according to previous research [13] as follows:

Where A represents the planting holes that contain the suspension with the culture medium. AC represents the control holes that contain the culture medium only. Then the strength of biofilm formation is calculated as follows:

$A \leq AC$ Non-biofilm forming

AC ≤ A ≤ 2 * AC  Medium biofilms
* 2AC ≤ A Strong biofilms

### The Effect of Calcium Nanoparticles on the Growth of Pathogenic Bacteria

Several concentrations of Calcim nanoparticles were prepared by dissolving 0.001 g of CaNPs and diluting them to achieve concentrations of 25 µg/ml, 50 µg/ml, 75 µg/ml, and 100 µg/ml, in accordance with previous research [14]. Four pathogenic bacterial species isolated from pathological cases—*P. aeruginosa*, *E. coli*, *K. pneumoniae*, and *S. aureus*—were tested in this study. The bacteria were cultured on Muller-Hinton agar, and wells with a diameter of 6 mm were created. A volume of 0.2 ml of the test concentrations was added to each well and incubated at 37 °C for 24 hours. After incubation, the diameters of the inhibition zones were measured using a numbered ruler [15].

### Prepare the Minimum Inhibitory Concentration (MIC)

A set of sterile test tubes was prepared, each containing 1.8 ml of nutrient broth medium. To this, 0.1 ml of bacterial suspension was added. Different concentrations of calcium nanoparticles (25 µg/ml, 50 µg/ml, 75 µg/ml, and 100 µg/ml) were introduced at a volume of 0.1 ml into separate tubes. Additionally, four control tubes were prepared with only the culture medium and bacterial suspension, without any calcium nanoparticles added; these served as negative controls. All tubes were incubated for 24 hours at 37°C. After incubation, the minimum inhibitory concentration (MIC) was determined by assessing the turbidity of the test tubes. The negative control tubes were compared with those containing bacterial cultures and varying concentrations of calcium nanoparticles to identify the lowest concentration that effectively inhibited bacterial growth [16]

### Effect of Calcium Nanoparticles on Catalase Enzyme

The test involved culturing the pathogenic bacterial species *P. aeruginosa*, *E. coli*, *K. pneumoniae*, and *S. aureus* in test tubes containing 1.8 ml of nutrient agar broth medium. To this, 0.1 ml of the minimum inhibitory concentration was added to four test tubes. Additionally, four test tubes containing only the culture medium and bacterial suspension served as negative controls. The tubes were then incubated at 37 °C for 24 hours. After incubation, a few drops were collected from both the treated and untreated bacterial cultures and placed on a sterilized glass slide. A few drops of 3% hydrogen peroxide solution were added, and the appearance of bubbles was observed [17].

### Detection of Inhibitory Activity of Nanoparticles (CaNPs) against Biofilm Forming Bacteria

The work was done according to method [18]. Biofilm-forming bacteria were activated on a nutrient-agar medium. Subsequently, 5 ml of Brain Heart Infusion broth medium containing 2% glucose was prepared in test tubes, into which the biofilm-forming bacteria were transferred. A 100-microliter aliquot of the bacterial suspension was added to each well of a standard plate for each bacterial isolate. The first well served as a control sample with no added nanoparticle concentrations. Next, 100 microliters of nanoparticle concentrations (ranging from 100 mg/g to 50 mg/g) were added to the remaining wells in a horizontal line, with three replicates for each bacterial isolate. The calibration plates were then incubated for 24 hours. After incubation, the contents of the wells were emptied and washed three times with a local phosphate buffer solution to remove non-attached bacterial cells. Crystal violet at a concentration of 3% was added to each well of the microtiter plate and allowed to sit for 15 minutes. Following this, 100 µl of 93% methanol was added, and the plate was left to dry for 10 minutes to fix the attached bacterial cells. The contents of each well were then emptied and washed with distilled water to remove any non-adherent dye, with this washing repeated three times. Finally, 160 µl of 33% glacial acetic acid was added, and the absorbance of the plate was measured at a wavelength of 630 nm using a Multiskan Go device. The following equation was then applied to determine the level of inhibition [19].

$$\text{Inhibition of biofilm formation} = \frac{\text{Wavelength of control pit} - \text{Wavelength of equation pit}}{\text{Wavelength of the control pit}} \times 100$$

## RESULTS AND DISCUSSION

### Sample Collection

Fifty-four soil samples were collected from various sites in northern Basrah, southern Iraq (Figure 1). These samples were gathered in sterilized plastic bottles by digging 5 cm into the soil with a shovel. The samples represented different types of soil, including agricultural, oil-polluted, riverbank, and those contaminated with animal dung, as detailed in Table 2. Specifically, samples were taken from sewage, the banks of the Tigris and Euphrates rivers, agricultural land, and oil-polluted areas (Table 3). The collection sites were primarily in the Al-Qurna and Al-Madinah districts in northern Basrah. The samples were transported to the laboratory within three hours of collection, labeled with information such as location, date, and type of soil. Under sterile conditions, 1 g of each sample was added to a test tube containing 10 ml of distilled water. Serial tenfold dilutions (10^-1 to 10^-5) of the samples were then prepared. Using a micropipette, 0.5 ml of each dilution was placed on nutrient agar plates, which were incubated overnight at 37 °C [20].

**Table 2** Sites and sorts of samples

| Site | Sort of soil samples | |
|---|---|---|
| sewage | 1 | Main outfall of Al-Midaina |
| | 2 | Central Processing unit of Al-Midaina |
| Farm soil | 3 | Bahla farms soil |
| | 4 | Northern Al-Midaina farms |
| River edge soil | 5 | Euphrates River edge soil |
| | 6 | Tigris River edge soil |
| Oil polluted soil | 7 | Rumaila oil field |
| | 8 | Drill 335 cutting soil |

| | | |
|---|---|---|
| Soil contaminated with animal dung | 9 | Soil contaminated with chicken dung |
| | 10 | Soil contaminated with animal dung |


**Fig. 1** the area of sample collection

**Table 3** The isolation sites, samples sorts, number of samples, and collection date

| No. | isolation site | samples sort | number of samples | collection date |
|---|---|---|---|---|
| 1 | sewage soil | Sewage of Al-Midaina | 8 | 18/9/2022 |
| 2 | | | | |
| 3 | River edge soil | Euphrates River/ Al-Midaina | 6 | 27 /9/2022 |
| 4 | Agricultural soil | Date palm farm | 8 | 7 /10/2022 |
| 5 | Pond soil | Weeds pond | 7 | 16 /10/2022 |
| 6 | Garden soil | Home garden | 5 | 27 /10/2022 |
| 7 | Oil contaminated soil | Northern Qurna field | 8 | 18 /11/2022 |
| 8 | Marsh soil | Zichri marsh | 5 | 18 /11/2022 |
| 9 | Dung contaminated soil | Barn | 7 | 28 /11/2022 |

## Diagnosis

### Microscopic Diagnosis

All bacterial isolates were purified, and staining of the bacteria showed that most of the bacteria were Gram-negative, i.e., 10 positive isolates (35.7%) and 18 negative isolates (64.2%).

### Phenotypic Diagnosis

The phenotypic characteristics for the initial diagnosis, as the shape, color, smell, texture, and size of the growing colonies were observed on the culture media of nutrient agar, blood agar, and MacConKy agar.

### Biochemical Tests

Biochemical tests were performed, and the test results were as shown in the table 4.

**Table 4** The biochemical tests

| Bacteria | Oxidase | MR | VP | Urease | $H_2S$ production | citrate | Gas production | Indole | Coagulase |
|---|---|---|---|---|---|---|---|---|---|
| *P. aeruginosa* | + | + | - | - | - | + | - | - | - |

### Molecular Diagnosis

Molecular identification of the bacterial isolates under study was carried out, and the PCR technique for the 16S rRNA gene was used to identify the bacteria [21]. The results of the DNA extraction of the bacteria showed the appearance of DNA bands that were extracted from the bacteria.

### Polymerase Chain Reaction (PCR)

After extracting the DNA from the bacterial isolates, the DNA was amplified using polymerase chain reaction (PCR). The amplification results showed that the DNA was at a size of 1400 bp when compared with the DNA ladder as shown in the figure 2.

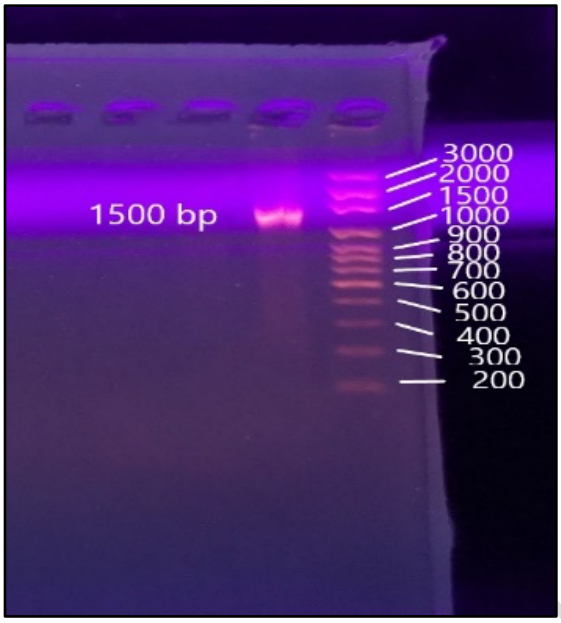


**Fig. 2** the DNA size of bacterial isolates and its comparison with the DNA ladder size index

### Genetic Sequencing Analysis

The SANQR technique was used to perform sequencing analysis resulting from the amplification of the 16rRNA gene. Blast analysis was also performed at NCBI Biotechology, and the bacterial isolate was registered at NCBI .and record under accession no PP273433.

### Biosynthesis of Nanoparticles

The present study showed that P *aeruginosa*. bacteria have the ability to biosynthesize nanoparticles of, CaNPs,. The properties of the synthesized nanoparticles were confirmed using the following techniques:

### Color Variation

The initial observations of nanobiosynthesis reveal color variations, with each material exhibiting distinct hues. For instance, the color range of calcium oxide varies from yellow to white in an emulsion, as illustrated in Figure 3. This color change in the composition may result from the excitation of surface plasmon vibrations in the nanoparticles, a defining characteristic of these materials [22]. Surface plasmon vibrations may arise from dipole oscillations when the electromagnetic field is in the visible range, resulting in collective oscillations of conduction electrons [23].

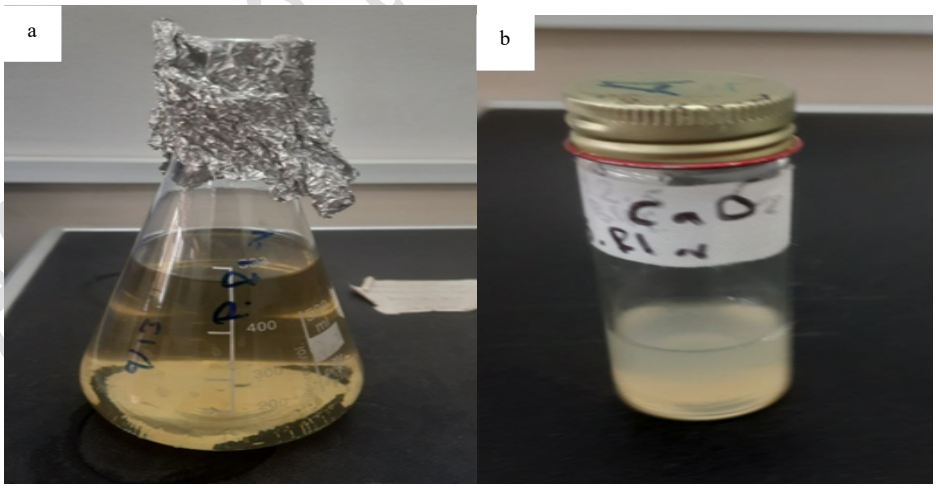


**Fig. 3** the color variation in solutions for each of the following: a) Bacterial suspension, b) Chromatic heterogeneity in calcium oxide

### UV-visible Spectroometer

The next step in verifying the synthesis of nanoparticles is to measure their wavelength, as each nanomaterial has a unique wavelength. For calcium oxide synthesis, the wavelengths range from 200 to 1000 nanometers, with peak absorption occurring at 318 nanometers, as illustrated in Figure 4. This result closely aligns with previous studies [6]. Proteins and enzymes, particularly the reduction enzyme present in the supernatant of bacterial cultures, play a crucial role in the biosynthesis of nanoparticles. The biological formation of nanoparticles, whether occurring inside or outside of cells, is influenced by the specific location where these particles are generated.

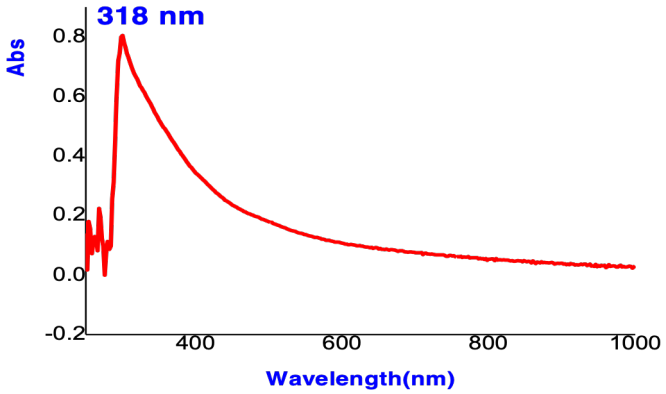


**Fig. 4** UV-visible spectra of calcium oxide nanoparticles produced by *P. aeruginosa*

## Fourier Trensmission Infrared Spectroscopy FTIR

The active groups present in the bacterial supernatant were detected using FTIR. These values were interpreted by entering them on the Inata NANO website, where the numbers are entered and the website identifies the active compounds and groups (Tables 5).

**Table 5** Active aggregates of CaNPs produced from the supernatant solution of *P. aeruginosa* bacteria

| FTIR of calcium nanoparticles formed from *P. arognosia* | | |
|---|---|---|
| Vehicles | Effective group | Peak (cm -1) |
| alcohol | O-H stretching | 3741.23 |
| alkyne | C-H stretching | 3266.82 |
| alkane | C-H stretching | 2923.56 |
| carbodiimide | N=C=N stretching | 2107.6 |
| alkyne | C≡C stretching | 2028.75 |
| cyclopentanone | C=O stretching | 1731.76 |
| alkene | C=C stretching | 1631.48 |
| nitro compound | N-O stretching | 1538.92 |
| alkane | C-H bending | 1450.21 |
| carboxylic acid | O-H bending | 1390.21 |
| aromatic ester | C-O stretching | 1238.08 |
| anhydride | CO-O-CO stretching | 1033.66 |

## SEM Examination

The shape, size, and surface morphology of the particles were analyzed using scanning electron microscopy (SEM). The SEM results for calcium oxide nanoparticles (CaNPs) synthesized through extracellular methods using *P.* bacteria revealed that the nanoparticles are composed of irregular granules, measuring approximately 13.08 nm in size, as illustrated in Figure 5. The nanoparticles, possessing a large surface area and high surface energy, tend to agglomerate. These findings align with previous studies [24]). The reason for the difference in the shape and size of the nanoparticles that are synthesized by biological systems is that this is a common matter [25]. The results of the current study were consistent with Study [26].

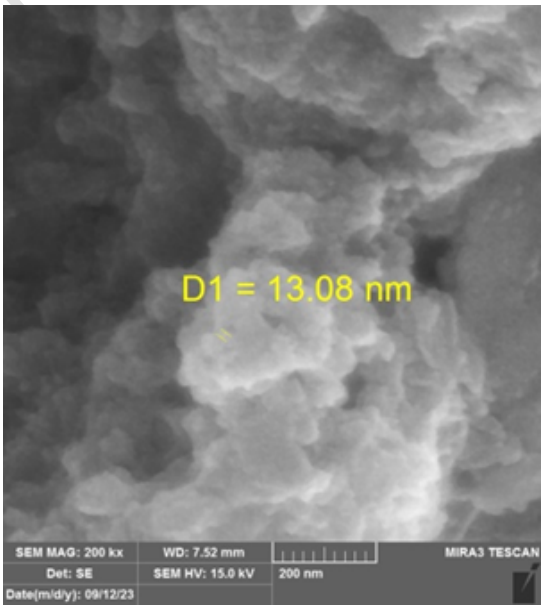


**Fig. 5** Electron microscope of calcium nanoparticles

### Detection of Biofilm Formation in Pathological Bacteria

The detection of biofilm-forming bacteria, which is considered a virulence factor, was carried out for four types of bacteria, namely *E. coli, K. penumonae, P. aeruginosa,* and *S. aureus*, using two methods:

### Congo Red Method

The bacteria were cultured on Congo red medium to determine if they formed biofilms. The results revealed the presence of black colonies, indicating that the bacteria produced biofilms with high intensity, as shown in Figure 6. These findings are consistent with previous research [8].

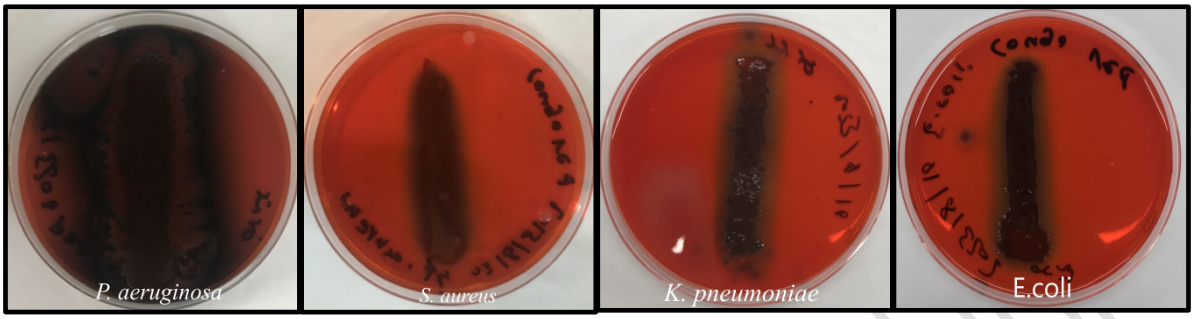


**Fig. 6** Detection of biofilms in pathogenic bacteria using Congo red agar

### Detection of Biofilms by a Standard Plate (Microtiter plate)

Biofilm-forming bacteria were detected using a microtiter plate. The ELISA results revealed that, by comparing the readings from the negative control well (which contained only culture medium) to those from the positive control well (which contained culture medium and bacterial colonies), the intensity of biofilm formation was calculated. All four isolates exhibited high-intensity biofilm formation, as shown in Table 6. This finding is consistent with previous studies [27].

**Table 6** Intensity of biofilm formation in pathogenic bacterial isolates by microtiter plate

| Bacteria | Biofilm intensity calculation equation | | Biofilm intensity |
|---|---|---|---|
| *P. aeruginosa* | 2 * AC ≤ A | 2 * 0.097 ≤ 1.135 | Strong biofilm |
| *E. coli* | 2 * AC ≤ A | 2 * 0.073 ≤ 1.511 | Strong biofilm |
| *K. pneumoniae* | 2 * AC ≤ A | 2 * 0.096 ≤ 1.164 | Strong biofilm |
| *S. aureus* | 2 * AC ≤ A | 2 * 0.106 ≤ 1.327 | Strong biofilm |

### Antimicrobial Activity of CaNPs

The results of the current study demonstrated that biosynthetic calcium nanoparticles (CaNPs) effectively inhibit the growth of pathogenic bacteria, exhibiting varying diameters of inhibition depending on the concentration used. The largest inhibition diameter was observed for *P. aeruginosa*, reaching 21 mm at a 100% concentration, while the smallest inhibition diameter was for *E. coli*, measuring 12 mm at a 25% concentration. These findings indicate that calcium nanoparticles, at different concentrations, can inhibit pathogenic bacterial growth to varying extents, as summarized in Table 7 and Figure 7. The data clearly show that bacterial growth inhibition occurs more significantly at higher concentrations. Additionally, there were notable differences in inhibition diameters among the bacterial isolates, attributed to variations in bacterial cell wall composition, overall cell physiology, genetic makeup, and the presence of enzymes critical to cellular metabolism [28].

**Table 7** Inhibition Zone (mm) on Pathogenic Bacteria

| Inhibition zone (mm) on Pathogenic Bacteria | | | | Pathogenic bacteria |
|---|---|---|---|---|
| concentration | concentration | concentration | concentration | - |
| 100 µg \ ml | 75 µg \ ml | 50 µg \ ml | 25 µg \ ml | - |
| 21 mm | 19.5 mm | 15.5 mm | 14.5 mm | *P. aeruginosa* |
| 14.5 mm | 14 mm | 12.75 mm | 12 mm | *E. coli* |
| 17 mm | 15.5 mm | 14.5 mm | 13.25 mm | *K. pneumonia* |
| 16 mm | 15 mm | 15 mm | 14 mm | *S. aureus* |

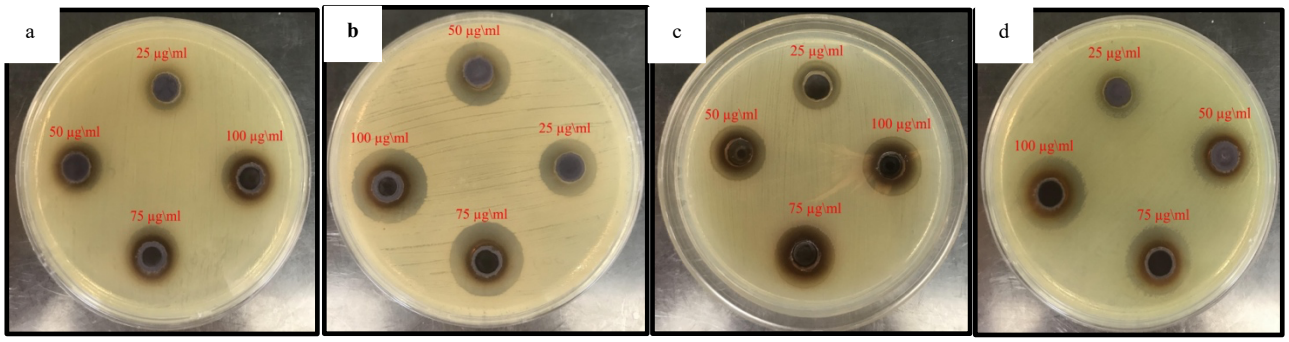


**Fig. 7** Effect of CaNPs on pathogenic bacteria a-*P. aeruginosa*; b-E. - *E. coli* c- *K. pneumonia* d- *S. aureus* with concentrations (25–50 - 75–100 µg/mL)

## Minimum Inhibitory Concentration (MIC)

The MIC results for *P. aeruginosa* E. coli K. pneumonia bacteria showed that it was 25 µg\ml while it was 50 µg\ml for *S. aureus* bacteria, as in the Figure 8.

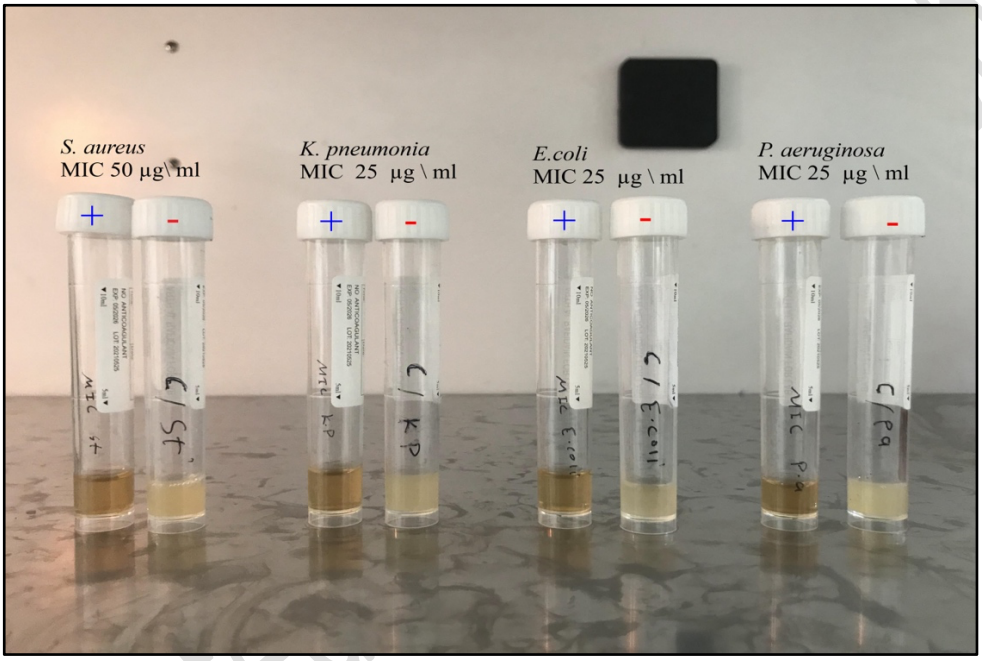


**Fig. 8** The minimum inhibitory concentration (MIC)

## Inhibition of Catalase Enzyme

The examination results indicated that Calcim nanoparticles at varying concentrations, as detailed in Table 8, effectively inhibited the production of the catalase enzyme in pathogenic bacteria. Catalase is a key virulence factor, as it helps bacteria decompose hydrogen peroxide into oxygen and water, protecting them from oxidative stress caused by reactive oxygen species (ROS). By overcoming oxidative stress, the catalase enzyme plays a crucial role in cellular defense. Meanwhile, the small size and positive charge of silver nanoparticles enable them to penetrate bacterial cells and disrupt biological molecules, ultimately leading to a reduction or complete absence of catalase production (see Figure 9) [29].

**Table 8** Concentrations of CaNPs on pathogenic bacteria inhibition catalase

| Inhibition concentration catalase | Isolate |
|---|---|
| 50 µg\ ml | *P. aeruginosa* |
| 25 µg \ ml | *E. coli* |
| 25 µg \ ml | *K. pneumonia* |
| 50 µg \ ml | *S. aureus* |

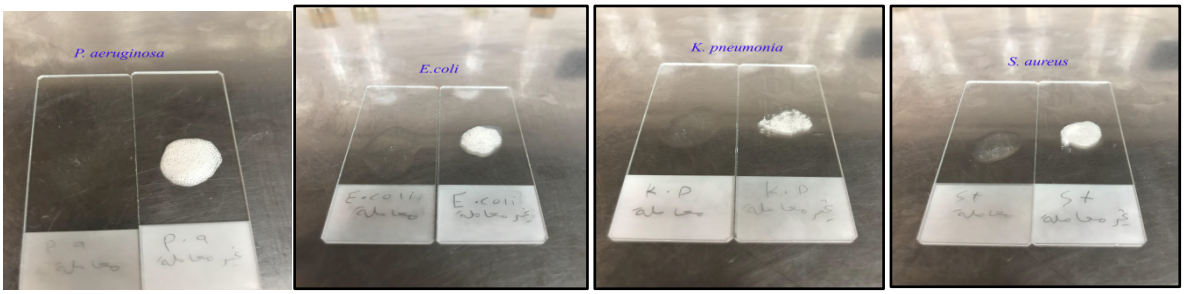


**Fig. 9** Inhibition catalase

### Inhibitory activity of calcium nanoparticles (CaNPs) against bacterial biofilms

The current study demonstrated that calcium nanoparticles (CaNPs) exhibit significant inhibitory activity against biofilm-forming bacteria, as detailed in Table 9. The highest inhibitory effect was observed against *S. aureus*, reaching 93.40% at a concentration of 100 µg/mL, while the lowest was against *P. aeruginosa*, which showed 86.80% inhibition at a concentration of 25 µg/mL. The findings indicate that CaNPs possess strong antibacterial properties due to their large surface area. Their small size enhances interactions with biofilm-forming bacteria, allowing the nanoparticles to penetrate bacterial cells easily. This penetration disrupts the cell membrane, ultimately leading to bacterial cell death [30].

**Table 9** Biofilm inhibition rate of CaNPs nanoparticles

| Average effect of Calcim nanoparticles | Average type of bacteria | Concentrations of Calcium nanoparticles | | | | Types of bacteria |
|---|---|---|---|---|---|---|
| | | 100 µg \ ml | 75 µg \ ml | 50 µg \ ml | 25 µg \ ml | |
| 88.05 | 87.80 | 89.53 % | 88.16 % | 87.77 % | 86.80 % | *P. aeruginosa* |
| 89.79 | 90.38 | 91.00 % | 90.53 % | 89.40 % | 91.07 % | *E. coli* |
| 90.49 | 91.63 | 92.57 % | 91.90 % | 91.30 % | 90.87 % | *K. pneumonia* |
| 91.37 | 89.90 | 93.40 % | 92.03 % | 91.70 % | 83.47 % | *S. aureus* |
| 4.506 Bilateral interference | | LSD 2.253 calcim nanoparticles | | | LSD 2.253 bacteria | |

## CONCLUSION

This study highlights that the biosynthesis of calcium nanoparticles (CaNPs) by *P.* bacteria is a straightforward, eco-friendly method. After confirming the characterization of the synthesized nanoparticles using UV, FTIR, and SEM, we observed that they were spherical in shape and varied in size, ranging from 29 to 40 nm. The findings demonstrate that these nanoparticles exhibit a strong inhibitory effect on biofilms formed by pathogenic bacteria and are effective as antibacterial agents and catalysts.

### Acknowledgments

The author who contributed to this work would like to thank the Department of Life Sciences, College of Education, Al-Qurna, and University of Basra for their great assistance and cooperation in completing this work.

## REFERENCES

1. Khajeh H., Fazeli-Nasab B., Pourshahdad A., Mirzaei A.R., Ghorbanpour M. Green-synthesized silver nanoparticles induced apoptotic cell death in *CACO2* cancer cells by activating *MLH1* gene expression. Scientific Reports. 2024; 14(1): 29601.
2. Samiei F., Fotoohiyan Z., Salehi-Sardoei A., Fazeli-Nasab B., Mirzaei A.R., Shafi N., Shameem N., Parray J.A. Biosynthesis of Silver Nanoparticles and Their Application in Agriculture. In Parray J A (Ed.), Progress in Soil Microbiome Research (pp. 259-302). Cham: Springer Nature Switzerland. 2024
3. Nosrati F., Fakheri B., Ghaznavi H., Mahdinezhad N., Sheervalilou R., Fazeli-Nasab B. Green synthesis of silver nanoparticles from plant Astragalus fasciculifolius Bioss and evaluating cytotoxic effects on MCF7 human breast cancer cells. Scientific Reports. 2025; 15(1): 25474.
4. Salary J., Matin H.H., Ghafari K., Hajati H. Effect of in ovo Injection of Calcium Carbonate Nanoparticles on Bone Post Hatched Characteristics and Broiler Chicken Performance. Iranian Journal of Applied Animal Science. 2017; 7(4): 663-667.
5. Hu X., Dang X., Shi T., Niu B., Zhang Q., Zheng L., Ni F. Potential Risk of Calcified Nanoparticles for Recurrent Urinary Tract Infection after Minimally Invasive Percutaneous Nephrolithotomy for Renal Calculi. Molecular and Cellular Biology (Noisy-le-grand). 2022; 68(3): 247-257.
6. Gandhi N., Shruthi Y., Sirisha G., Anusha C. Facile and eco-friendly method for synthesis of calcium oxide (CaO) nanoparticles and its potential application in agriculture. The Saudi Journal of Life Sciences. 2021; 6: 89-103.
7. Sambrook J., Russell D.W. Purification of nucleic acids by extraction with phenol: chloroform. Cold Spring Harbor Protocols. 2006; 2006(1): pdb. prot4455.
8. Hamady S.R., Abbass I.J., Kadhim K.F. Detection of Biosynthesis of CuNPs using P. aeruginosa Isolated from Soil. International Journal of Biotech Trends and Technology-IJBTT. 2024; 14.
9. Kamnev A.A., Dyatlova Y.A., Kenzhegulov O.A., Vladimirova A.A., Mamchenkova P.V., Tugarova A.V. Fourier transform infrared (FTIR) spectroscopic analyses of microbiological samples and biogenic selenium nanoparticles of microbial origin: Sample preparation effects. Molecules. 2021; 26(4): 1146.
10. Ma H., Shieh K.-J., Qiao T.X. Study of transmission electron microscopy (TEM) and scanning electron microscopy (SEM). Natural Science. 2006; 4(3): 14-22.
11. Mori S., Yamada A., Kawai K. Evaluation of the biofilm detection capacity of the Congo Red Agar method for bovine mastitis-causing bacteria. Japanese Journal of Veterinary Research. 2024; 71(3): 109-116.
12. Almeida C., Azevedo N.F., Santos S., Keevil C.W., Vieira M.J. Discriminating multi-species populations in biofilms with peptide nucleic acid fluorescence in situ hybridization (PNA FISH). PloS one. 2011; 6(3): e14786.
13. Tang J., Kang M., Chen H., Shi X., Zhou R., Chen J., Du Y. The staphylococcal nuclease prevents biofilm formation in Staphylococcus aureus and other biofilm-forming bacteria. Science China Life Sciences. 2011; 54(9): 863-869.

14. bakht Dalir S.J., Djahaniani H., Nabati F., Hekmati M. Characterization and the evaluation of antimicrobial activities of silver nanoparticles biosynthesized from Carya illinoinensis leaf extract. Heliyon. 2020; 6(3).
15. Saliminasab M., Jabbari H., Farahmand H., Asadi M., Soleimani M., Fathi A. Study of antibacterial performance of synthesized silver nanoparticles on Streptococcus mutans bacteria. Nanomedicine Research Journal. 2022; 7(4): 391-396.
16. Furqon I.A., Hikmawati D., Che A.C.A. Antibacterial properties of silver nanoparticle (AgNPs) on stainless steel 316L. Nanomedicine Research Journal. 2021; 6(2): 117-127.
17. Patil S.V., Borase H.P., Patil C.D., Salunke B.K. Biosynthesis of silver nanoparticles using latex from few euphorbian plants and their antimicrobial potential. Applied Biochemistry and Biotechnology. 2012; 167(4): 776-790.
18. Mathur T., Singhal S., Khan S., Upadhyay D., Fatma T., Rattan A. Detection of biofilm formation among the clinical isolates of staphylococci: an evaluation of three different screening methods. Indian Journal of Medical Microbiology. 2006; 24(1): 25-29.
19. Namasivayam S.K.R., Preethi M., Bharani A., Robin G., Latha B. Biofilm inhibitory effect of silver nanoparticles coated catheter against Staphylococcus aureus and evaluation of its synergistic effects with antibiotics. International Journal of Biological & Pharmaceutical Research. 2012; 3(2): 259-265.
20. Mulamattathil S.G., Bezuidenhout C., Mbewe M., Ateba C.N. Isolation of environmental bacteria from surface and drinking water in Mafikeng, South Africa, and characterization using their antibiotic resistance profiles. Journal of Pathogens. 2014; 2014(1): 371208.
21. Janda J.M., Abbott S.L. The genus Aeromonas: taxonomy, pathogenicity, and infection. Clinical microbiology reviews. 2010; 23(1): 35-73.
22. Hashim M. Study the Antibacterial Activity of Gold Nanoparticles against Some Clinical Isolates. PhD Thesis, M. Sc. thesis, department of biology, college of science. 2018
23. Kalathil S., Lee J., Cho M.H. Electrochemically active biofilm-mediated synthesis of silver nanoparticles in water. Green Chemistry. 2011; 13(6): 1482-1485.
24. Tiwari M., Jain P., Hariharapura R.C., Narayanan K., Bhat U., Udupa N., Rao J.V. Biosynthesis of copper nanoparticles using copper-resistant Bacillus cereus, a soil isolate. Process Biochemistry. 2016; 51(10): 1348-1356.
25. Joseph A.T., Prakash P., Narvi S. Phytofabrication and characterization of copper nanoparticles using Allium sativum and its antibacterial activity. International Journal of Science Engineering and Technology. 2016; 4(2): 463-472.
26. Yaaqoob L. Evaluation of the biological effect synthesized iron oxide nanoparticles on Enterococcus faecalis. Iraqi Journal of Agricultural Sciences. 2022; 53(2): 440-452.
27. Kunwar A., Shrestha P., Shrestha S., Thapa S., Shrestha S., Amatya N.M. Detection of biofilm formation among Pseudomonas aeruginosa isolated from burn patients. Burns Open. 2021; 5(3): 125-129.
28. Jadhav V., Bhagare A., Wahab S., Lokhande D., Vaidya C., Dhayagude A., Khalid M., Aher J., Mezni A., Dutta M. Green synthesized calcium oxide nanoparticles (CaO NPs) using leaves aqueous extract of moringa oleifera and evaluation of their antibacterial activities. Journal of Nanomaterials. 2022; 2022(1): 9047507.
29. Roy S., Das T.K. Effect of biosynthesized silver nanoparticles on the growth and some biochemical parameters of@@ Aspergillus foetidus. Journal of Environmental Chemical Engineering. 2016; 4(2): 1574-1583.
30. Ramola B., Joshi N.C., Ramola M., Chhabra J., Singh A. Green synthesis, characterisations and antimicrobial activities of CaO nanoparticles. Oriental Journal of Chemistry. 2019; 35(3): 1154.